Low- and high-frequency vibration isolation for scanning probe microscopy

1998 Meas. Sci. Technol. 9 383

(http://iopscience.iop.org/0957-0233/9/3/011)

Meas. Sci. Technol. **9** (1998) 383–390. Printed in the UK PII: S0957-0233(98)86286-3

Low- and high-frequency vibration isolation for scanning probe microscopy

A I Oliva†‡, M Aguilar† and Víctor Sosa§

† Instituto Ciencia de Materiales, CSIC, Campus Universidad Autónoma, Cantoblanco, 28049, Madrid, Spain
§ CINVESTAV-IPN Unidad Mérida, Departamento de Física Aplicada, AP 73-Cordemex, 97310, Mérida, Yucatán, Mexico

Received 25 July 1997, accepted for publication 17 November 1997

Abstract. A study of the vibration isolation system in scanning probe microscopes (SPMs) to reduce external noises in a wide range of frequencies is presented. For the low-frequency isolation case, a pneumatic system based on a cylindrical plastic tube with an elastic membrane for damping is studied. The theoretical model and the experimental results obtained from it to isolate noises above 2 Hz are discussed. For the high-frequency isolation, a design based on stacked metallic sheets, with cylindrical elastomers (viton) between them, is simulated. The effect of the elastomer geometry when it is used in a real case by means of the transfer function of the vibration system is discussed. From the results, we are able to predict and optimize the performance of SPMs with regard to noise isolation.

1. Introduction

Since the invention of the surface analysis techniques based on a probe located with high precision, such as the scanning tunnelling microscope (STM), the atomic force microscope (AFM), the magnetic force microscope (MFM) and others (called globally scanning probe microscopes, SPM), a lot of devices designed to suppress external noises have appeared [1–3]. The vibration isolation system (VIS) plays a very important role in the SPM design, so it is important to study its performance. This stem from the necessity of controlling the extremely short distance between the sample and the probe. Since a SPM is usually exposed to external vibrations at various frequencies, it is necessary to reduce these noises to get better results. However, a single VIS capable of cutting off noises at all frequencies does not exist. This makes it necessary to use various systems to isolate SPMs from external noises. External noises that affect these techniques can be divided into two groups: *low- and high-frequency* noises.

Typical *low-frequency* noises that disturb the analysis are usually below 100 Hz; common sources are people walking or talking, floor and building resonances, electrical lines, doors openings and closing and others. For low-frequency isolation, scientists have used sand boxes, tyres, metallic springs holding devices from the roof, superconductor levitation, eddy-current dampers, optical tables and other devices. The first two are always cheaper and they are optimized by *trial and error*. Optical tables can support big loads and reduce the noise down to 0.5 Hz, but they are not cheap. New designs of ultra-low-frequency isolation based on a crossed wire pendulum [4] and a folded pendulum [5] have recently been proposed in order to reduce the cut-off frequency to some millihertz for seismometer applications.

For the *high-frequency* noises, it is necessary to use other isolation designs, such as the acoustical chambers and elastic elements (such as elastomers) used generally in compact SPMs. Noises at these frequencies, usually above 100 Hz, come from mechanical pumps, cooling systems and mechanical tools working around the site. Normally, it is easy to reduce high-frequency noises by using an elastomer, but noise isolation is neither quantified nor controlled. Starting with the design of the *pocket-size* STM [6], which is isolated from vibrations with an elastomer material made of viton, several compact systems with their SPMs mounted in small closed spaces, such as vacuum and/or cryogenic chambers, have been proposed.

In this work, two vibration isolation designs to reduce the low- and high-frequency noises are analysed separately. For the reduction of a low-frequency noise system based on a cylindrical tube with an elastic membrane for damping is used. We discuss the proposed theoretical model and the experimental results obtained from it to isolate noises down to 2–3 Hz. For the high-frequency isolation, a design based on stacked metallic sheets with a small amount of elastomer between them is studied. The effect of the elastomer dimensions on the VIS performance is

‡ Permanent address: CINVESTAV-IPN Unidad Mérida, AP 73-Cordemex, 97310, Mérida, Yucatán, Mexico.

discussed. The *cut-off frequency* is determined by a theoretical model which uses parameters obtained from experiments. Transfer function plots help us to visualize the level of noise reduction. As far as we know, this work is the first study done to propose a set of two isolator devices which, together, help to reduce noises in a wide range of frequencies for SPM applications.

2. The low-frequency system

2.1. A description of the device

The VIS for low frequency consists of a group of four similar cylinders connected together, to support the four corners of a base. In this way, each cylinder supports a quarter of the weight applied on the base. Each cylinder is made of plastic PVC of 20 cm height and 15 cm diameter (figure 1). The cylinder is divided by a plate into two chambers: the upper one called the *spring chamber* and the bottom one called the *damping chamber*. This divisor plate has a small hole in the centre to permit the flow of air between the two chambers (the damping effect) when the VIS is working. An elastic membrane (0.5 cm thick) is used to close and seal the upper chamber and it is fixed with screws and bolts through a circular edge. The *load support* is located in the centre of the elastic membrane. This load support is formed by two PVC circular plates (called buttons) which have a hole in the centre. The elastic membrane is pressed and sealed between these two buttons by means of a screw through its centre. The *button* diameter determines the size of the membrane area used for isolation. A base is located into the cylinder to support the load when the cylinder is not inflated. This helps to avoid unnecessary deformations in the elastic membrane. Air is introduced into the damping chamber through a valve. Therefore, the load is supported by air through the elastic membrane and an oscillating and damping effect is obtained when a sudden vibration occurs. The frequency of these oscillations is measured through a connector in the damping chamber and it is used to experiment with various air pressures. A plastic transparent tube filled with water is coupled to this connector as a water column, to measure the air pressure applied into the chamber.

2.2. Theory

Each vibrating system has several natural frequencies of oscillation and, when it is affected by an external excitation at this frequency, a resonant response is obtained. A method to prevent resonances in SPM is to design the mechanical system of the SPM such that its natural resonant frequencies stay far from frequencies of the common external vibrations. However, to reach this goal, we need to analyse each component involved and study its effect on the whole system.

A typical one-dimensional vibration system (a harmonic oscillator) includes three main parameters: the mass M, stiffness constant K and damping coefficient C. The system will respond depending on the values of K and C of the elastic material. If the relation $[C/(2M)]^2 < K/M$ holds, that is, $K > C^2/(4M)$, then the motion is always a damped oscillation [7], with amplitudes $x(t)$ varying according to

$$x(t) = x(0)\cos(\omega t)\exp[-Ct/(2M)] \tag{1}$$

where $x(0)$ is the initial amplitude and $\omega = \{(K/M) - [C/(2M)^2]\}^{1/2}$ the frequency of oscillation. The amplitude $x(t)$ follows an exponential decrement modulated by a harmonic function. This behaviour can be experimentally demonstrated by locating a sensor (a piezoelectric device, for example) on the upper stage of the SPM. The response of the system when it is perturbed with a weak push (by hand) can be recorded on an oscilloscope, as Okano *et al* [8] demonstrated. Measuring the maximum amplitudes $x_m(t)$ from the evolving curve of this damped response permits one to calculate the damping factor C by means of the relation

$$C = -(2M/t)\ln[x_m(t)/x(0)] \tag{2}$$

which was obtained from equation (1).

For the case of this low-frequency device, when a load is applied on the *load support* (through the *button*), the elastic membrane suffers a deformation. The air volume displaced depends on the geometry acquired by the membrane and the radius of the *button* used. We introduce the concept of the *effective area*, A_{eff}, of the elastic membrane defined as an area such that its product with the vertical displacement h produced by the load yields the total volume displaced by the elastic membrane. If the membrane is only slightly deformed by the internal pressure, then a linear deformation can be assumed, like a disc with the load support at the centre (see figure 1). Thus, the volume displaced by this deformation is given by

$$V = \pi l^2 h - 2\pi \int_l^{l_i} x f(x)\,\mathrm{d}x \tag{3}$$

where l is the radius of the cylinder, l_1 the radius of the *button*, h the vertical displacement of the *button* and $f(x)$ represents the deformation of the elastic membrane. Taking a simple straight line deformation model,

$$f(x) = \left(\frac{h}{l-l_1}\right)x - l_1\left(\frac{h}{l-l_1}\right) \tag{4}$$

then equation (3) gives

$$V = \pi\left(l^2 h - \frac{2h(l^3 - l_1^3)}{3(l-l_1)} + \frac{hl_1(l^2 - l_1^2)}{l-l_1}\right) \tag{5}$$

and from its previous definition the effective area is obtained:

$$A_{eff} = \pi\left(l^2 - \frac{2(l^3 - l_1^3) - 3l_1(l^2 - l_1^2)}{3(l-l_1)}\right). \tag{6}$$

If the *effective area* is expressed in terms of the cross sectional area of the cylinder ($A = \pi l^2$) namely, $A_{eff} = \delta A$, then this δ factor can be written as

$$\delta = 1 - \frac{2(l^3 - l_1^3) - 3l_1(l^2 - l_1^2)}{3(l-l_1)l^2}. \tag{7}$$

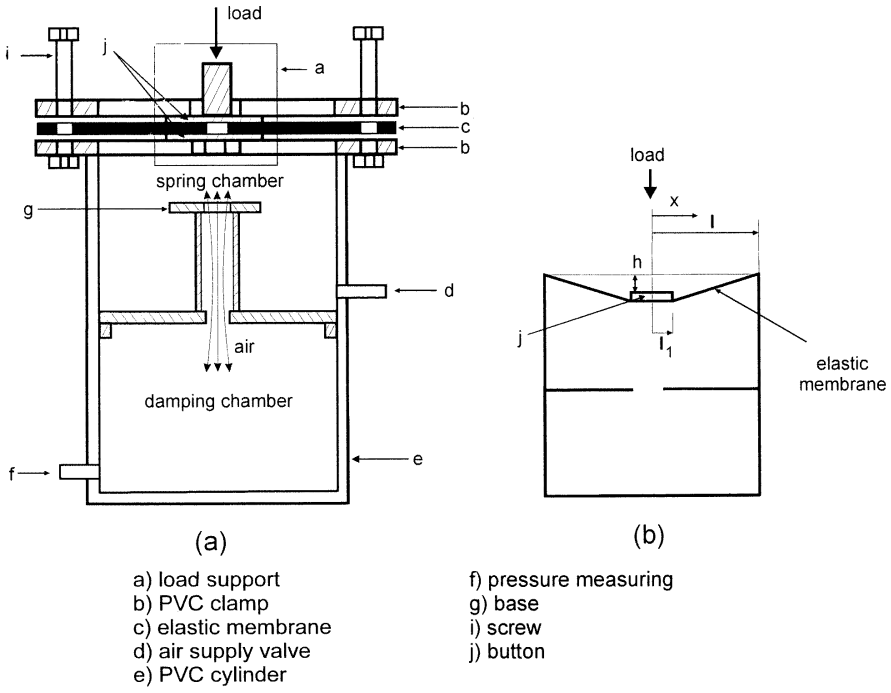

Figure 1. The low-frequency isolator. (a) A cross sectional view of the pneumatic isolator analysed. (b) The linear deformation model used for the theoretical analysis of the isolator.

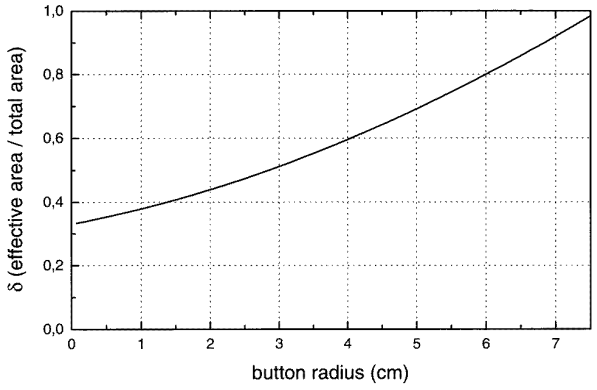

Figure 2. The δ factor as a function of the *button* radius l_1 calculated with equation (7).

Figure 2 shows the δ factor as a function of the *button* radius l_1 for a cylinder of radius $l = 7.5$ cm. Clearly, the *effective area* does not increase linearly with the *button* radius.

Now, by using the concept of the *effective area*, we can find the *net force* F_{net} in the centre of the *button*, $F_{net} = \Delta P A_{eff}$. In the upwards direction, the difference in pressures ΔP is given by

$$\Delta P = P_i - P_{atm} - \frac{F_{ext}}{A_{eff}} \tag{8}$$

where P_{atm} is the atmospheric pressure and F_{ext} represents the external force or load on the system. The internal pressure P_i (composed of the atmospheric pressure P_{atm} and the applied pressure on the cylinder) can be obtained from the ideal gas equation $P_i = nRT/V_T$, where n is the number of moles of gas in the cylinder, R the ideal gas constant, T the absolute temperature and V_T the total volume of the spring chamber. Thus, by substitution into equation (8), the net force F_{net} is given by

$$F_{net} = \frac{nRT}{V_T} A_{eff} - P_{atm} A_{eff} - F_{ext} \tag{9}$$

considering the first term on the right-hand side of equation (9) as the most important. Then, by differential calculus, we obtain finally

$$\mathrm{d}F_{net} = -\frac{P_i}{V_T} (A_{eff})^2 \, \mathrm{d}h. \tag{10}$$

From this last equation, the stiffness constant K of the whole isolator system is defined as

$$K = \frac{P_i}{V_T} (A_{eff})^2. \tag{11}$$

This last equation shows that, if we increase P_i, we will increase the stiffness constant K; but, if we increase the size (volume) of the cylinder, the K value will decrease. Therefore, we can obtain a certain value of the resonant frequency only by changing the internal pressure or by changing the volume of the chamber. Roughly, the corresponding resonance frequency can be found with the well known relationship

$$\omega = (K/M)^{1/2} \tag{12}$$

M being the mass of the system.

2.3. Experimental work

In order to measure the frequency of oscillation for various air pressures on the chamber, a set-up based on a lever whose fulcrum is at one end was implemented. A known load is applied to the other end, such that, at a certain distance along the lever, the load support is fixed; thus, the real load value directly applied to the elastic membrane can be easily calculated. The internal pressure P_i of the chamber is measured with the height that the water column reaches for each applied load. Once the water column's height is stable, the valve is closed to isolate the water column from the cylinder. Now, we give a small perturbation by hand to produce an oscillation and to measure its frequency. This process is repeated for various air pressures (water column heights) and various loads. Finally, we plot this frequency as a function of the applied loads. Loads of 250, 300 and 400 N were applied to the load support. Similar experiments were performed by changing the diameter of the *button* (5, 7.5 and 12.7 cm), namely the *effective area*. More controlled experiments were realized by perturbing the STM's base when it was working (under tunnelling conditions). The tunnelling current signal stays stable when no perturbation affects the base. A controlled vibration produced by an eccentric load fixed on a DC motor axis for unbalancing was applied to the STM's base as a perturbation. Changes in the tunnelling current signal were measured as a function of the vibration frequency (several motor velocities) when the perturbation was applied. These results were compared with the stable condition.

3. The high-frequency system

3.1. A description of the device

The elastomer *viton* has elastic properties, as well as chemical stability, and it is usually used as a material for high- and ultra-high-vacuum seals. For high-frequency isolation, we used sets of three pieces of cylindrical *viton*, as material for high-frequency vibration isolation. We cut these pieces from commercial 'O' rings, in various lengths and diameters. Three cylindrical viton pieces were symmetrically circled between two metallic, ring-shaped sheets, which are parts of the mechanical system of our VIS–SPM design. The VIS consists of several stages (metallic plates) separated by the viton elements. The sensor probe (the tip–sample junction, in the case of STM, or the lever–surface junction, in the case of AFM) is on the upper stage. A detailed view of the metallic plates and the arrangement of the viton pieces on them is presented in figure 3. Note that the cylindrical vitons are horizontally positioned such that forces act radially on them.

3.2. Theory

High-frequency noise is easy to reduce by simple methods. However, it is necessary to know the properties of the materials involved in the design in order to quantify the level of isolation. In a previous work [9], a theoretical method to calculate the transfer function of an isolator

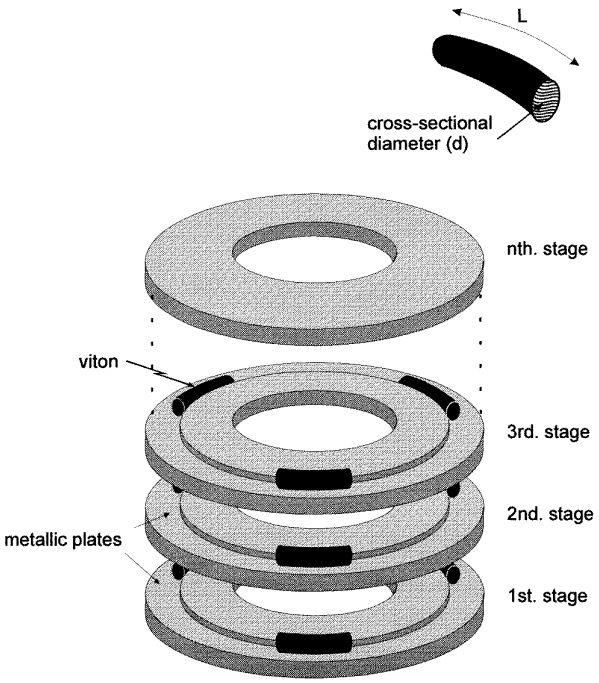

Figure 3. The high-frequency isolator. The viton geometry and the metallic plates arrangement is shown. The diameter *d* and length *L* of the viton are the parameters analysed in this work.

system composed of several metallic stacks separated with viton (elastomer) between them was proposed. In this arrangement, each stage reduces the noise from the base to the upper stage. Therefore, the level of noise on the upper stage can be predicted if we know the properties of the elastomer. Here, we propose a method to measure the elastic properties of various geometries of this elastomer widely used in compact SPMs. These properties were used to simulate the transfer function under several arrangements.

Previously, we reported a graphical method to study the effects of M, K and C in a multi-stage VIS with one-dimensional motion [10]. This method proved to be very useful to predict the response of the mechanical system of a SPM built of six stages. In that case, we obtained a *cut-off frequency* of 800 Hz for a transfer function of -120 dB, which is still very high for practical purposes. One recommendation for obtaining very high resolution in an SPM is to design the device in such a way that the noise amplitude in the upper stage be less than 1 pm (10^{-12} m) with a *cut-off frequency* as small as possible. Therefore, it is necessary to reduce the resonance frequency response of the VIS as much as possible.

Our results will be discussed in terms of the model presented earlier [10]. According to this model, the transfer function (expressed in decibels) of the VIS is defined as

$$\mathrm{dB} = 20\log(x_n/Y_0) \tag{13}$$

and represents the relationship between the amplitude of oscillation of the final nth stage x_n and the amplitude of the external noise Y_0 as a function of the excitation

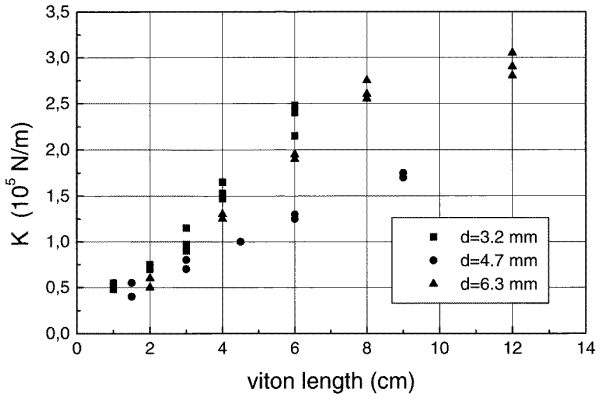

Figure 4. The stiffness constant K measured as a function of the length of viton. Constant K was obtained for three diameters d of viton. A nearly linear behaviour was obtained in each case.

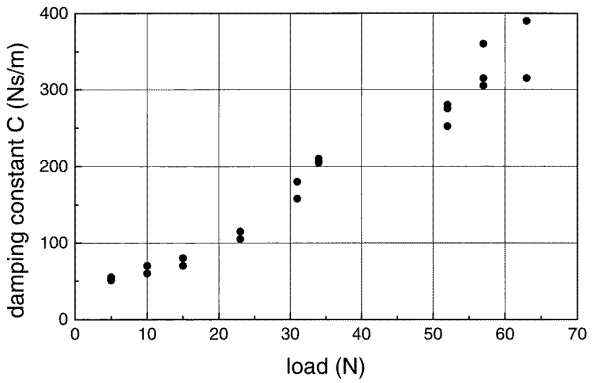

Figure 5. Experimental results obtained for the damping constant C for a single stage and three vitons with d = 4.7 mm and L = 5 mm. C increases when the applied load increases. Values obtained are in agreement with those reported in the literature.

frequency. To perform a more realistic simulation, we used experimental data to adjust the parameters of the model. In all cases, we assumed an arbitrary value of $Y_0 = 10^{-6}$ m, so we needed to reduce x_n to six orders of magnitude below Y_0; that is, we sought dB $= -120$ dB. This arbitrary value could be converted into a real value if the noise amplitude and frequency of the room were known. Similarly, this simulation gives real orders of magnitude in the noise reduction.

3.3. Experimental work

The effects of various cross sectional diameters (d) and lengths (L) of viton were investigated in this work. In particular, the following values were used: $d = 3.2$, 4.7 and 6.3 mm and L in the range 5–60 mm.

The value of the stiffness constant K of viton was determined by using a single stage (a metallic plate over the three vitons). A load F was applied to the system and the consequent displacement Δx was measured with a digital micrometer once the system had reached stability. According to Hooke's law, K is given by the slope of the F versus Δx plot. The load applied to the set-up was less than 50 N. Within this range, a linear behaviour of K was always found. With higher loads, non-linearity of K was observed. This non-linearity behaviour needs to be considered if the static load on viton is higher than 50 N. In this work we are interested in compact SPMs, for which the plates used for vibration isolation are lighter than 50 N. K values were plotted as functions of d and L. Figure 4 shows these results. A nearly linear dependence of K on L is observed. Large lengths yields higher values of K. Different slopes were obtained for different values of d; the smallest corresponded to $d = 4.7$ mm. For values of L greater than 10 cm, K was no longer found to be linear. These last results allow us to predict for design considerations, in this range, a value of K for a given L.

Since viton is a viscoelastic material, it also has a damping coefficient C. This parameter was obtained with the same experimental set-up as for the determination of K. For that, a weak push was given by hand to the base. The responses obtained, using a piezoelectric sensor located on the top of the plate, were measured. We used a Tektronix 7623A oscilloscope with memory to record the temporal oscillation curves. Measuring the relation between two consecutive amplitudes and the time between them, we calculated, by using equation (2), the damping coefficient C of the set-up. Figure 5 shows the results obtained for C as a function of the applied load; they are in agreement with the values reported by other authors [8].

4. Results

4.1. Low frequency

Figure 6(a) shows the theoretical natural frequency of the low-frequency isolator as a function of the internal pressure in the chamber, for various loads and button diameters as calculated from the equation (12). Note that the frequency response increases for higher pressures. Masses of 25, 30 and 40 kg and button diameters of 5.1, 7.6 and 12.7 cm were used for calculations. On comparing the curves obtained, it can be seen that the frequency response decreases for high loads (or masses) and low button diameters.

Figure 6(b) summarizes the experimental results obtained with the low-frequency isolator. These results are comparable with the theoretical results shown in figure 6(a) because the same conditions were used. Here, the oscillation frequencies obtained when various loads were applied to a single damper cylinder with different *button* diameters are shown. The frequency responds linearly with the internal pressure applied in a similar way to that in figure 6(a). For a given value of *button* diameter, the frequency decreases when the applied load increases. We found also that the natural frequency increases as the *button* diameter increases. Therefore, theoretical data agree with the experimental results.

Real effects were measured in an STM under tunnelling conditions. A known vibration in frequency was introduced in the base of the STM by means of an unbalanced DC motor. With this perturbation, changes in the tunnelling current were recorded when the chambers were inflated

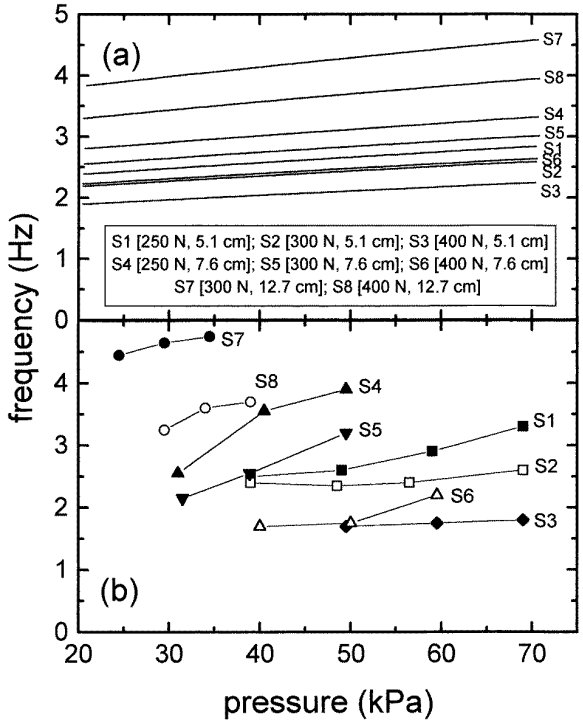

Figure 6. (a) Theoretical results of the *cut-off frequency* obtained for the low-frequency VIS as a function of the internal pressure P_i. Values of loads and *button* diameters used are shown in the inset. (b) Experimental results obtained by measuring the natural frequency of the low-frequency VIS, as a function of P_i, for the same values of loads and *button* diameters as those in (a). Experimental results exhibit similar behaviour to that obtained in the theoretical simulation.

and deflated. The fast Fourier transform (FFT) of the captured signal was calculated to get the intensity of the perturbations. The result is shown in figure 7 for the case of a 25 Hz vibration. Full lines show the response obtained from the tunnelling current when the isolation was absent (chambers deflated). The dotted line is the response of the tunnelling current when the isolation system was working (chambers inflated). The main frequency at 25 Hz and its harmonics can be seen clearly. In this case, the amplitudes were reduced by about a factor of 20 when the isolation system was used. Various experiments were performed with different motor frequencies. At frequencies lower than 25 Hz the isolation effect was small. On the other hand, at frequencies higher than 25 Hz, the signal was also small but, because of the effect of the *cut-off frequency* of the STM feedback loop used to maintain the tunnel current constant. In this case it is important to remark upon the level of isolation reached, considering the simple design used. Commercial systems can give higher isolation values but with very high costs.

4.2. High frequency

Once information about the elastic properties of viton had been obtained, it was possible to estimate the behaviour of a real system consisting of several stacks. The results for a

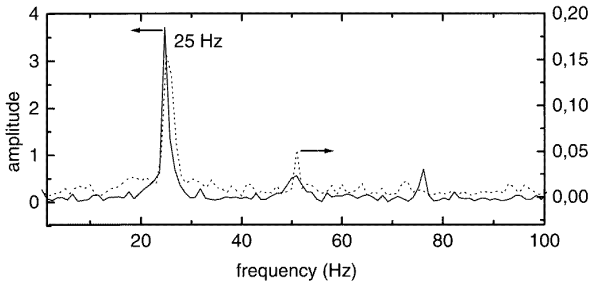

Figure 7. The FFT response of the tunnelling current when the system is perturbed with a vibration of 25 Hz. The full line is the response without the isolator (chamber not inflated) and the dotted line is the response when the isolator is working (chamber inflated). The low-frequency noise was reduced by a factor of about 20.

VIS of seven stages, separated by viton elements (diameter 4.7 mm) are presented in figure 8. The mass of the first six stages was 0.208 kg and the upper mass was 1.5 kg. Four curves are shown, corresponding to different lengths of viton. Curve a illustrates the response of the last stage when a complete 'O' ring is used between each ring-shaped sheet (perimeter 390 mm). It can be seen that poor isolation is obtained, giving an extremely high frequency for the -120 dB level (not shown in figure 8). Therefore, this arrangement would not be useful for the isolation system designed in this work. Curves b, c and d show the responses of the last stage when we used a set of three vitons between each plate. The three curves correspond to 20, 10 and 5 mm viton length, respectively. We will call the frequency reached at this level (-120 dB), the *SPM cut-off frequency*. One can draw the conclusion that, as L diminishes, the cut-off frequency diminishes too. For curve d, the *SPM cut-off frequency* is about 340 Hz. However, there is a practical limitation for viton lengths, because of stability. Also, it is necessary to have a parameter d at least of the same size as the parameter L, otherwise the system becomes mechanically unstable. Calculations in figure 8 were performed using $C = 80$ N s m^{-1} as a representative value for the viton used, taken from figure 5.

A similar result was obtained for viton pieces with the same values for M and C and a larger cross sectional diameter ($d = 6.3$ mm), as can be see in figure 9. In this case, the response with an entire 'O' ring is not shown. In order to make a comparison, viton lengths were selected such that we obtained the same d/L ratio in both figures. It can be seen in figure 9 that SPM *cut-off frequencies* are slightly larger than those obtained with $d = 4.7$ mm. From the last two figures we can conclude that the best result is obtained with the lowest value of L and consequently the lowest value of K.

On the other hand, we can study the effect of mass on the transfer function. For a VIS of seven stages, the first two masses were of 0.624 kg, the third and fourth masses of 0.416 kg, the fifth and sixth masses of 0.208 kg and the seventh (top) mass of 1.5 kg. We used viton pieces with $d = 4.7$ mm and $L = 5$ mm, values that optimized our results with identical masses. The idea of this arrangement was to decrease the mass of the stage as

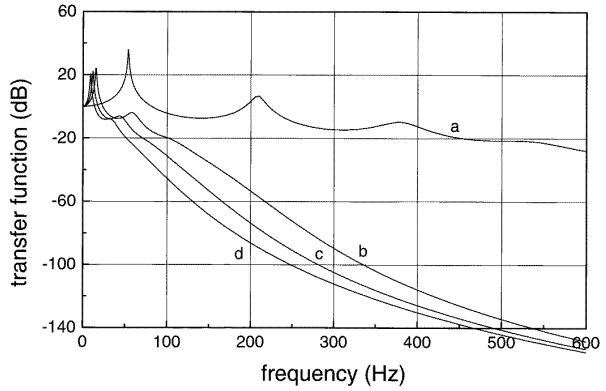

Figure 8. The transfer function of the last stage of a seven-stage VIS system obtained with a viton diameter d = 4.7 mm for four viton lengths. The first six masses are equal to 0.208 kg and M_7 = 1.5 kg. Curve (a) corresponds to an entire 'O' ring (L = 390 mm) used between plates. Other curves used the following viton lengths (L): (b) 20 mm, (c) 10 mm and (d) 5 mm. K values were (a) 1516400 N m^{-1}, (b) 123300 N m^{-1}, (c) 71800 N m^{-1} and (d) 42000 N m^{-1}. A typical value of C = 80 N s m^{-1} was taken for all curves.

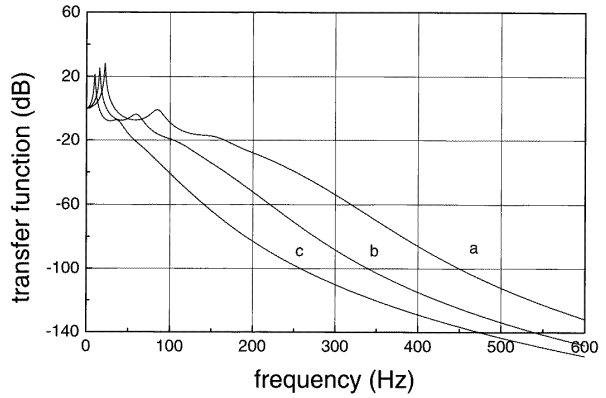

Figure 9. Similar to figure 8 but with a viton diameter d = 6.3 mm. Here, we used the same d/L ratio as that in figure 8. L values were (a) 26.6 mm, (b) 13.3 mm and (c) 6.6 mm. K values used for calculation were (a) 255100 N m^{-1}, (b) 127600 N m^{-1} and (c) 50600 N m^{-1}. We used C = 80 N s m^{-1} in all cases.

the height increases, the uppermost mass being the probe–sample stage.

With this set-up, we obtained a better isolation of the SPM from external noise. Figure 10 shows the transfer functions of some stages of this set-up. The SPM *cut-off frequency* on the last (seventh) stage has been lowered to $\simeq$250 Hz (for -120 dB). Identical results were obtained when the order of masses is inverted and the seventh mass kept equal to 1.5 kg. The other curves show how isolation performance improved from stage to stage.

The number of stages is another parameter to analyse. When the number is decreased, the SPM *cut-off frequency* increases and the best solution is to increase the mass of the remaining stages.

The high-frequency VIS proposed here is currently being used at atmospheric pressure, but it is possible to use it under high-vacuum conditions. As can be seen, this system does not work in the low-frequency range. Therefore, we must use another isolation set-up in this frequency region, such as the pneumatic device discussed before.

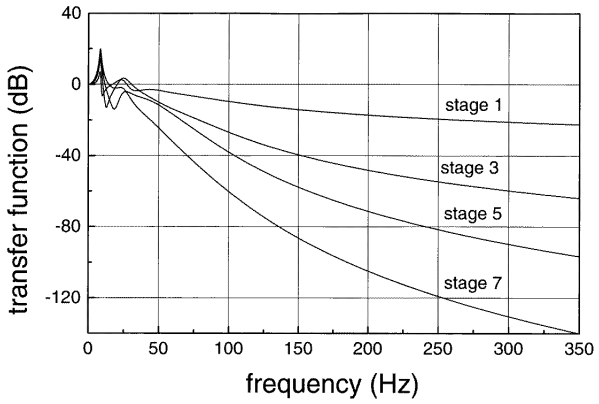

Figure 10. Transfer functions of some stages of a seven-stage VIS when the positions and values of the masses were exchanged (d = 4.7 mm). In this case, $M_1 = M_2$ = 0.624 kg, $M_3 = M_4$ = 0.416 kg, $M_5 = M_6$ = 0.208 kg and M_7 = 1.5 kg. With this arrangement we obtained a *cut-off frequency* of 250 Hz (-120 dB). For simulation, K = 42100 N m^{-1} and C = 100 N s m^{-1} were used.

5. Conclusions

The performance of a very cheap low-frequency isolation system based on a pneumatic cylindrical chamber has been discussed. Experimental results agreed with the results from a simple theoretical model developed for this cylindrical geometry. This isolation system is being used now as four cylinders connected together and supporting an STM/AFM head. With this arrangement we increased the chamber volume and the response time for sudden perturbations.

For the case of the high-frequency isolator, the elastic properties of viton as an element for vibration isolation were studied. A system consisting of several metallic stages, stacked and isolated from each other by means of the viton pieces, was simulated. By changing the diameter and length of the viton pieces, the response in frequency was optimized and we found that the best results were obtained with the lowest length and an optimized distribution of masses of the metallic stages. A method to measure the elastic constant K and damping constant C in order to use real properties in the VIS simulation was presented. We demonstrated that the high-frequency noise can be lowered by 120 dB down to 250 Hz, by means of a seven-stage VIS arrangement.

Acknowledgments

A I Oliva thanks the CONACYT (Mexico) for the grant given during his postdoctoral fellowship at the ICMM-CSIC, Spain. We appreciate the technical assistance given by E Corona, O Ceh and F J Espinosa-Faller during this work.

References

[1] Binnig G and Rohrer H 1982 Scanning tunneling microscope *Helv. Physica Acta* **55** 726

[2] Binnig G, Quate C F and Gerber Ch 1986 Atomic force microscope *Phys. Rev. Lett.* **56** 930

[3] Pohl D W 1986 Some design criteria in scanning tunneling microscopy *IBM J. Res. Dev.* **30** 417

[4] Kanda Noboyuki, Barton M A and Kazuaki Koruda 1994 Transfer function of a crossed wire pendulum isolation system *Rev. Sci. Instrum.* **65** 3780

[5] Liu Jiangfeng, Winterflood J and Blair D G 1995 Transfer function of an ultralow frequency vibration isolation system *Rev. Sci. Instrum.* **66** 3216

[6] Gerber Ch, Binning G, Fuchs H, Marti O and Rohrer H 1986 Scanning tunneling microscope combined with scanning electron microscope *Rev. Sci. Instrum.* **57** 221

[7] Thompson W T 1982 *Teoría de Vibraciones* (New York: Prentice Hall International)

[8] Okano M, Kajimura K, Wakiyama S, Sakai F, Mitzutani F and Ono M 1987 Vibration isolation for scanning tunnelling microscope *J. Vac. Sci. Technol.* A **5** 3313

[9] Oliva A I, Sosa V, De Coss R, López-Salazar N, Sosa R and Peña J L 1992 Análisis de un sistema de aislamiento de vibraciones usando un método gráfico *Rev. Méx. Fís.* **38** 497

[10] Oliva A I, Sosa V, De Coss R, López-Salazar N, Sosa R and Peña J L 1992 Vibration isolation analysis for scanning tunneling microscope *Rev. Sci. Instrum.* **63** 3329